



# A novel pectin/cerium (IV) silicomolybdate-based nanocomposite ion exchanger: preparation, characterization, and applications

Sugandhi Gupta<sup>1</sup> · Esmat Laiq<sup>1</sup> · Uzma Meraj<sup>1</sup>

Received: 4 March 2023 / Accepted: 7 August 2023 / Published online: 28 August 2023  
© Iran Polymer and Petrochemical Institute 2023

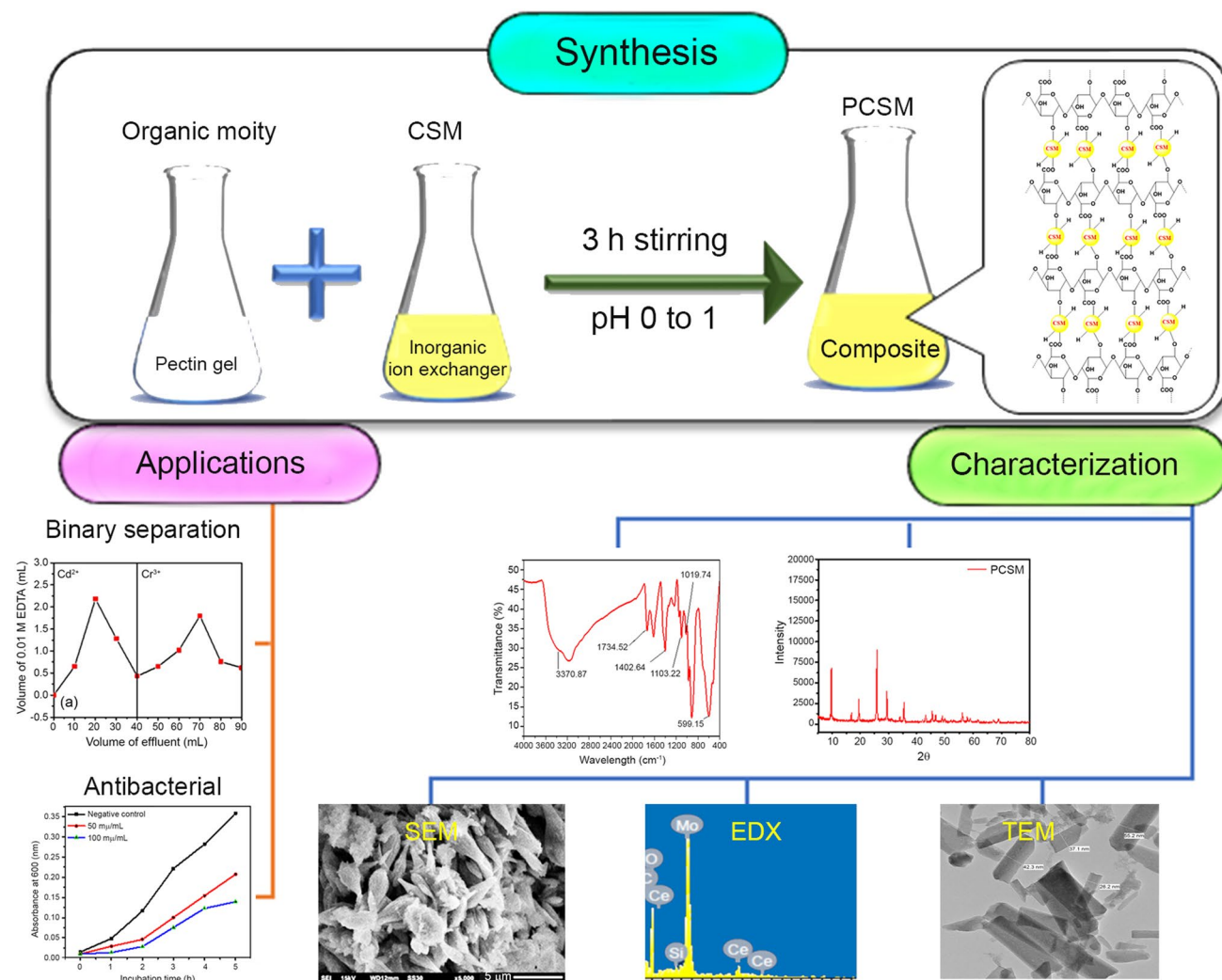
## Abstract

Hybrid ion exchangers with high ion exchange capacity (IEC), good stability, and good selectivity for heavy metals formed through a polymer material into an inorganic ion exchanger have always attracted the attention of researchers. In this work, a novel nanocomposite ion exchanger made of pectin and cerium (IV) silicomolybdate (CSM) was synthesized by precipitation technique and used for separating heavy metals and eliminating bacterial pollutants from water systems. The structural and morphological investigation of the synthesized pectin–cerium (IV) silicomolybdate (PCSM) was achieved by Fourier transform infrared spectroscopy (FTIR), X-ray diffractometry (XRD), transmission electron microscopy (TEM), and scanning electron microscopy (SEM) techniques, whereas, its chemical characterization was performed by energy-dispersive X-ray (EDX) spectroscopy. The IEC, and chemical and thermal stability of the composite were also determined to understand the composite material's properties. The IEC of the PCSM and CSM was 2.56 and 1.78 milli equivalents per g, respectively. PCSM exhibited chemical stability against different chemical solutions and was thermally stable at 600 °C and retained 24.21% of its initial IEC. The distribution coefficient ( $K_d$ ) values of the numerous investigated metallic ions were assessed using different solvents to determine the composite's ion exchange characteristics. The distribution study indicated that PCSM was more selective toward  $\text{Cr}^{3+}$  ions. In addition, it was found to be effective for the separation of  $\text{Cr}^{3+}$  ions from binary metal ion mixtures such as  $\text{Cd}^{2+}$ – $\text{Cr}^{3+}$ ,  $\text{Pb}^{2+}$ – $\text{Cr}^{3+}$ ,  $\text{Ni}^{2+}$ – $\text{Cr}^{3+}$ , and  $\text{Co}^{2+}$ – $\text{Cr}^{3+}$ . PCSM has also shown antibacterial activity against Gram-negative bacteria *Escherichia coli*.

✉ Esmat Laiq  
esmat.wc@amu.ac.in

<sup>1</sup> Department of Chemistry, Aligarh Muslim University,  
Aligarh 202002, India

## Graphical abstract



**Keywords** Composite · Ion exchanger · Pectin biopolymer · Distribution studies · Antibacterial studies

## Introduction

Due to growing industrialization and urbanization, environmental degradation has become a real issue. Industries and residences emit enormous amounts of organic and inorganic contaminants into water systems. Carbon-based pollutants such as phenolic compounds, insecticides, and pesticides severely affect the environment [1]. In addition, due to their potential carcinogenic effects, they deteriorate the underground water quality and affect human health once discharged into the environment [2]. On the other hand, lead, cobalt, chromium, cadmium, and many more heavy metals have significant health risks and must be purged before being released into the water, soil, or air [3]. These heavy metal ions are actively utilized in various industries,

including electroplating, metallurgy, tanning, wood preservation, pulp and paper making, and paints and pigments manufacturing which contaminate and harm biological and ecological creatures. Therefore, metal differentiation is essential for understanding how metal ions behave in the environment. For example, Cr (VI) has been found to be harmful to people even though Cr (III) is not a significant environmental contaminant [4]. The environment's plentiful oxygen causes Cr (III) to be oxidized into Cr (VI), which is highly water soluble and potentially poisonous [5]. The presence of metal ions in an environment that exceeds the permitted limit is the source of severe health problems and even cancer [6, 7]. Coagulation [8], photocatalysis [9], ion exchange [10], reverse osmosis [11], adsorption [12], and other chemical and physical procedures are employed to

remediate water-containing metallic pollutants [13]. Because of its broad applicability, improved selectivity, and cost-effectiveness in wastewater treatment processes, distribution by ion exchange materials has attracted people's curiosity for using this strategy [14, 15].

Nature has endowed us with a wide range of inorganic and organic ion exchange materials, each with unique characteristics and selectivity. Inorganic ion exchangers provide several advantages over organic resins, including better chemical and thermal stability at high temperatures. Nevertheless, inorganic ion exchangers have some drawbacks too, such as unsuitability for column operation because of their high cost, non-granulometric nature, irreproducibility of the results [15]. On the other hand, organic ion exchangers are cost-effective, produce reproducible results, and can treat of a large amount of wastewater. Therefore, composite ion exchange materials have received much attention because they combine the desirable features of their organic and inorganic counterparts in a single material [16]. Because of their specificity, selectiveness, and wide pertinence, composite ion exchangers are utilized for environmental cleanup [17].

Among various composites, fibrous ion exchangers based on thorium (IV) and cerium (IV) have versatile characteristics that make them very important in industrial and environmental applications [18]. Such materials have new applications in fuel cells, ion-selective electrodes, antimicrobial activity, ion transport, ion exchange, catalysis, etc. [19–21]. Additionally, biocomposite ion exchangers that combine the advantages of biopolymers and inorganic materials have drawn increased interest as adsorbents for removing various contaminants because of their organizational and functional abilities [22, 23]. Biopolymers like gum acacia, chitosan, cellulose acetate, and pectin have been incorporated as organic polymer components in biocomposites ion exchangers [24–26]. Many research studies have shown that pectin and pectin-rich materials have a high affinity for metallic ions, and thus act as effective biosorbents [27]. The performance of the composite's ion exchange is enhanced by the inclusion of various carboxyl and hydroxyl groups, which increase the active sites on the surface of the polymer matrix [28]. So, pectin-based composite ion exchangers have been shown to interact efficiently with inorganic compounds through molecular associations, and due to their fibrous nature, abundance, and broad surface area. Some pectin-based ion exchangers such as pectin–cerium tungstate, pectin cerium iodate, and pectin zirconium silicophosphate have shown the selectivity toward  $Zn^{2+}$ ,  $As^{3+}$ ,  $Cu^{2+}$ , and  $Th^{4+}$ , respectively [29–31]. But, to the best of our knowledge and as per our detailed literature survey, there is no available data on the preparation of pectin–cerium (IV) silicomolybdate (PCSM) composite ion exchanger that shows higher selectivity for  $Cr^{3+}$  ions and antimicrobial activities commonly exhibited from transition metals with organic moieties [32].

So, the synthesis of hybrid materials through chemical methods signifies one of the most captivating improvements in material chemistry [33–35].

The current study focuses on the following objectives: preparation of cerium (IV) silicomolybdate (CSM) and PCSM composite ion exchanger, its characterization, and its practical use as a metal adsorbent to remove toxic metals from water sources, as well as its antibacterial activity against Gram-negative bacteria *Escherichia coli*. Such studies of hybrid ion exchangers encourage the synthesis of multifunctional ion exchangers and may cause a substantial impact on underground water purification.

## Experimental

### Materials

For our experiments, pectin and chromium chloride ( $CrCl_3$ ) were purchased from Loba Chemie (Loba Chemie Pvt. Ltd., Mumbai, India). Whereas, ammonium ceric nitrate ( $(NH_4)_2Ce(NO_3)_6$ ), cadmium chloride ( $CdCl_2$ ), lead nitrate ( $Pb(NO_3)_2$ ), barium nitrate ( $Ba(NO_3)_2$ ), ethylene diamine tetra acetic acid (EDTA) potassium hydroxide (KOH), sodium hydroxide (NaOH), sodium chloride (NaCl), hydrochloric acid (HCl), perchloric acid ( $HClO_4$ ), sodium perchlorate ( $NaClO_4$ ), and ammonium molybdate ( $(NH_4)_6Mo_7O_{24}$ ) were purchased from Fisher Scientific (Fisher Scientific India Pvt. Ltd., Mumbai, India). Sodium silicate ( $Na_2SiO_3$ ) was purchased from Otto Chemie (Otto Chemie Pvt. Ltd., Mumbai, India) and acetic acid ( $CH_3COOH$ ) was purchased from Merck (Merck, Darmstadt, Germany). The nickel nitrate ( $Ni(NO_3)_2$ ), magnesium nitrate ( $Mg(NO_3)_2$ ), zinc nitrate ( $Zn(NO_3)_2$ ), strontium nitrate ( $Sr(NO_3)_2$ ), ferric nitrate ( $Fe(NO_3)_3$ ), calcium nitrate ( $Ca(NO_3)_3$ ), cobalt nitrate ( $Co(NO_3)_3$ ), nitric acid ( $HNO_3$ ), and acetone ( $CH_3COCH_3$ ) were obtained from Central Drug House (Central Drug House Pvt. Ltd., New Delhi, India). Demineralized water (DMW) was procured from the lab itself and used for different solution preparation.

### Instrumentation

First, the magnetic stirrer (2 MLH, Remi, Maharashtra, India) was used to well mix the calculated amount of chemicals. Thereafter, a digital Systronics pH meter-361 (Meter-361, Systronics, Gujrat, India) was used to measure the solutions' pH. To observe various functional groups in the synthesized composite, we have used Fourier transform infrared spectroscopy (FTIR) technique. In this technique, the spectrum of the composite material was obtained by FTIR spectrophotometer (Spectrum Two FTIR spectrometer, PerkinElmer, Waltham, USA) using the KBr disc method.

Furthermore, we used a standard optical system for the data collection over the range of 4000 to 400  $\text{cm}^{-1}$ . It also serves standard configuration of atmospheric vapor compensation. The X-ray diffractometry (XRD) studies were conducted by X-ray diffractometer (D8 advance, Bruker AXS Inc., Madison, USA). The X-ray patterns of the composites were recorded using Cu-K $\alpha$  radiation with the wavelength 1.54 Å (corresponding energy is 8.04 keV) in the 2 $\theta$  angle range from 5° to 80°. The step size and the smoothing width were 0.02° and 0.3°, respectively, along with the step time of 6.00 s. Thereafter, the morphology of the composite was examined using a scanning electron microscopy (SEM) (JSM 6510LV, JEOL Ltd., Tokyo, Japan). The energy-dispersive X-ray (EDX) spectroscopy with 20 kV accelerated voltage was performed to obtain the elemental composition of the composite with the help of the same equipment, JEOL-JSM 6510LV scanning electron microscope (JSM 6510LV, JEOL Ltd., Tokyo, Japan). Moreover, the particle size was determined by capturing TEM images using a transmission electron microscope (TEM2100, JEOL Ltd., Tokyo, Japan). After the characterization, we also examined the desired applications such as ion exchange capacity (IEC) and antibacterial activity. Therefore, to determine the ion exchange capacity of the synthesized composite, glass columns were used. To examine the growth curve of *Escherichia coli*, the absorbance was measured as a function of incubation time through an UV-2600i spectrophotometer (UV-2600i, Shimadzu Corporation, Kyoto, Japan).

### Preparation of cerium (IV) silicomolybdate (CSM)

The CSM was synthesized by constantly agitating an aqueous  $\text{Na}_2\text{SiO}_3$  solution and boiling  $(\text{NH}_4)_2\text{MoO}_4$ . By adding 0.1 M  $\text{HNO}_3$  into the solution, the pH was adjusted in the range of 0–1. Thereafter,  $(\text{NH}_4)_2\text{Ce}(\text{NO}_3)_6$  was added to this mixture. Then the mixture was kept under constant stirring for 3 h. The digestion of the compound was performed for 24–25 h at room temperature. The liquid was decanted, and the precipitate was washed with DMW and dried in a laboratory oven at  $60 \pm 2$  °C. The compound was converted to  $\text{H}^+$  form by soaking in one molar  $\text{HNO}_3$  for a day with periodic shaking and repeatedly changing the supernatant with new acid. Finally, the solution filtration was done, and the precipitate was washed repeatedly with DMW to remove excess acid [36].

### Preparation of the pectin–cerium (IV) silicomolybdate (PCSM) composite ion exchanger

Pectin gel was obtained by dissolving various quantities of pectin powder in DMW. Furthermore, PCSM was prepared by mixing pectin gels with CSM. The mixture was maintained at 55 °C for 3 h on a magnetic stirrer. The resulting

light-yellow color precipitate was left at room temperature for 24 h until being digested. The gel was filtered after the supernatant was decanted. The surplus acid was washed away with DMW and processed at 55 °C in an air oven. The product was processed with 1.0 M  $\text{HNO}_3$  for 24 h with periodic stirring and the replacement of the supernatant liquid with new acid to convert the dried product to the  $\text{H}^+$  form. After many washes using DMW, the surplus acid was removed and the product was left to dry at 60 °C in an oven [36].

### Ion exchange capacity (IEC)

Basically, ion exchange is a process in which the ions present in any aqueous solution are removed/replaced by the other ions attached to the exchanger. To measure the ability of the exchanger in exchanging the desired ion, we commonly examine the IEC of composite toward the specific metal ion in a particular solution. In our experiments, the column method was adopted to study the IEC of the material by placing 1.0 g of  $\text{H}^+$  type exchanger in a 1.0 cm diameter glass column. NaCl solution was used to extract the hydrogen ions. The collected effluent was then titrated with 0.1 M solution of NaOH. As per Eq. (1), the IEC (in meq/g) was calculated as [37]:

$$\text{IEC} = \frac{av}{w}, \quad (1)$$

Here “ $a$ ” represents the molarity (mol/L) of the alkali, “ $v$ ” represents the volume (mL) of the alkali applied in the titration, and “ $w$ ” represents the exchanger's weight (g).

### Impact of eluent concentration and the behavior of elution on IEC

The effectiveness of the column and the optimal eluent concentration required to remove  $\text{H}^+$  ions from PCSM was found by passing 250 mL of NaCl (having different concentrations) with a flow rate of 1.0 mL/min through a column containing 1.0 g of PCSM. The collected effluents were subjected to a 0.1 M NaOH solution for titration. Now, as per the observation of IEC for different concentrations of NaCl, 1.0 M concentration of NaCl was found to be suitable for studying elution behavior. Therefore, 1.0 M NaCl was used to elute the  $\text{H}^+$  ions from the PCSM completely. The effluent was collected in segments of 10 mL at a set flow rate and to calculate the  $\text{H}^+$  ions that were eluted out of the column, effluents were titrated against a solution of 0.1 M NaOH.

### Thermal studies

As it is well known, polluted wastewater from industries is hot. So, hybrid ion exchangers should be thermally stable

for utilizing them in the purification of polluted wastewater treatment. Hence, we studied the effect of various temperatures on the IEC of synthesized PCSM composite. The influence of heat on the IEC of PCSM was investigated by placing 1.0 g of the composite in  $H^+$  form in the muffle furnace at a temperature ranging from 100 to 600 °C for 1 h. Then after the cooling PCSM, the IEC of the samples was calculated by the column method as discussed in the “ion exchange capacity” section [38].

### Chemical stability

The chemical stability of PCSM in various chemical solutions such as mineral acids (HCl,  $HNO_3$ ), alkalis (KOH, NaOH), and solvents (like acetone and acetic acid) was investigated through the chemical dissolution process. In this procedure, 0.5 g of PCSM was equilibrated with 50.0 mL of several chemical solutions for 24 h at room temperature. Then the excess acid, base, and other solutions were removed by washing and filtering. The remaining PCSM was washed with DMW and then dried to 60 °C. The chemical stability of PCSM was examined through the change of its color and weight. Eventually, the column method (or batch method) was used to calculate the IEC again.

### Distribution studies

Distribution studies were performed to gauge the relative selectivity of the PCSM ion exchanger toward specific ions in particular solvents. Herein, the ion exchanger is considered to be highly selective for an ion in a particular solvent if the values of the distribution coefficient ( $K_d$ ) are relatively larger for it. The batch approach was used to conduct distribution tests for several metal ions. In this technique, 0.4 g of PCSM exchanger in the form of  $H^+$  ions were added into 40 mL of different metallic solutions. Thereafter, to achieve the equilibrium, the mixtures were kept for 6 h at room temperature ( $\sim 25 \pm 2$  °C) under continuous shaking. After achieving the equilibrium, concentrations of these metal ion solutions were analyzed by titrating them with EDTA. The volumetric determination was performed by taking the metal ion's initial and final concentrations after equilibrium. The values of distribution  $K_d$  were computed using Eq. (2) [39]:

$$K_d = \frac{I - F}{F} \times \frac{V}{W} \quad (2)$$

The starting volume of the EDTA titrant is “ $I$ ” (mL), the final volume is “ $F$ ” (mL), the volume of the metal ions in mL is “ $V$ ”, and the weight of the exchanger is “ $W$ ” (g).

### Binary separation

On the PCSM ion exchanger, binary separation of various metal ions was performed using the column method [40]. In this procedure, a glass column (with an internal diameter of 1.0 cm) with a glass wool support at the bottom was packed with 1 g of PCSM in the  $H^+$  form. Subsequently, the column was washed once or twice with DMW. Then the mixture of various metal ions (5 mL of 0.01 M metal ion solution) that is to be separated was loaded by passing it (flow rate 1.0 mL/min) through the column. This mixture was passed through the column at least four or five times for the complete adsorption of metal ions by PCSM. Now considering the  $K_d$  values of various metal ions present in different solvents on the PCSM column, different eluents were used to elute the metal ions adsorbed on the exchanger. Any metal ion having low  $K_d$  in a particular solvent elute first as they are weakly held in PCSM composite while metal ion having high  $K_d$  in some solvent elute second as they are strongly held in PCSM composite in comparison to former. Each 10 mL portion of the effluent was collected at a flow rate of 5–6 drops/min. Finally, the titrimetric method was used to quantify the metal ions in effluent using a 0.01 M disodium salt of EDTA.

### Antibacterial activity

For a long time, microbial infections caused by several bacteria have been a foremost challenge in front of medical as well as sanitation industries [41]. In this study, the antibacterial activity of PCSM composite was examined against the bacteria *Escherichia coli*. For this purpose, the optical density technique was used to determine the antibacterial activity of the PCSM composite. First, *Escherichia coli* was aerobically grown in NB (nutrient broth) at 37 °C for 24.0 h. Thereafter, 13% of NB was autoclaved after being prepared in DMW. The bacterial culture was introduced to 100 mL DMW in the three individual flasks. Then 50.0 and 100.0  $\mu\text{g/mL}$  of PCSM were added to the bacterial culture in two separate flasks, while the third one remained without an ion exchanger. The bacterial culture without the treatment of PCSM was considered as a negative control. The flasks were placed in an incubator shaker at  $37 \pm 1$  °C. To monitor the bacterial concentration, 3 mL of suspension was taken from every flask to assess the optical density at 600 nm. The growth curve was plotted by taking optical density at 1 h intervals [30].

### Results and discussion

The optimum ratio of the distinct reagents composing the CSM has to be determined. Consequently, various compositions of ammonium ceric nitrate, ammonium molybdate,

and sodium silicate were tested to estimate the suitable CSM composition that yields the highest CSM's IEC (Table 1). CSM-3 exhibited the highest IEC (1.78 meq/g) among the prepared CSM compounds (Table 1), it was, thus, chosen to

**Table 1** Composition and some properties of the prepared CSM and PCSM ion exchanger composites

S. no.	Samples	Mixing volume ratio				Color	Na <sup>+</sup> IEC (meq/g)
		A	B	C	D		
1	CSM-1	1	1	1	–	Yellow	1.23
2	CSM-2	1	1	2	–	Yellow	1.14
3	CSM-3	1	2	1	–	Yellow	1.78
4	CSM-4	2	1	1	–	Faded yellow	0.99
5	PCSM-1	1	2	1	1	Faded yellow	1.98
6	PCSM-2	1	2	1	2	Faded yellow	2.56
7	PCSM-3	1	2	1	3	Faded yellow	2.02

Maximum deviation in IEC of all CSM and PCSM composites is  $\pm 2\%$

A = 0.1 M  $(\text{NH}_4)_2\text{Ce}(\text{NO}_3)_6$

B = 0.1 M  $(\text{NH}_4)_6\text{Mo}_7\text{O}_{24}\cdot 4\text{H}_2\text{O}$

C = 0.1 M  $\text{Na}_2\text{SiO}_3\cdot 9\text{H}_2\text{O}$

D = Pectin gel in DMW

synthesize the PCSM inorganic–organic hybrid ion exchange of different compositions by mixing distinct quantities of pectin and CSM-3. It can also be observed from Table 1 that the mixing of pectin into CSM results in an improved IEC. This may be explained on the basis of higher active sites available on the surface area of the composite. The main reason for this observation can be rooted in the binding of organic polymer (pectin) with the inorganic moiety (CSM) that not only provide the mechanical strength and active sites for combining the replaceable  $\text{H}^+$  ions but also prevent dribbling of composite from columns [40]. Figure 1 shows the schematic illustration of the proposed chemical reaction, and hence the formation of PCSM. Apart from it, further addition of pectin beyond a specific concentration may cause a decrement in IEC due to the accumulation of active sites served by higher concentrations of pectin. Here in our case, according to the composite IEC analysis given in Table 1, PCSM-2 has a higher IEC (2.56 meq/g) compared to the other combinations and is better than its inorganic analog as well, calculated under similar conditions. Therefore, the sample having this combination (PCSM-2) was chosen for further investigations.

We have also determined the thermal stability of PCSM by examining changes of its IEC and color as a

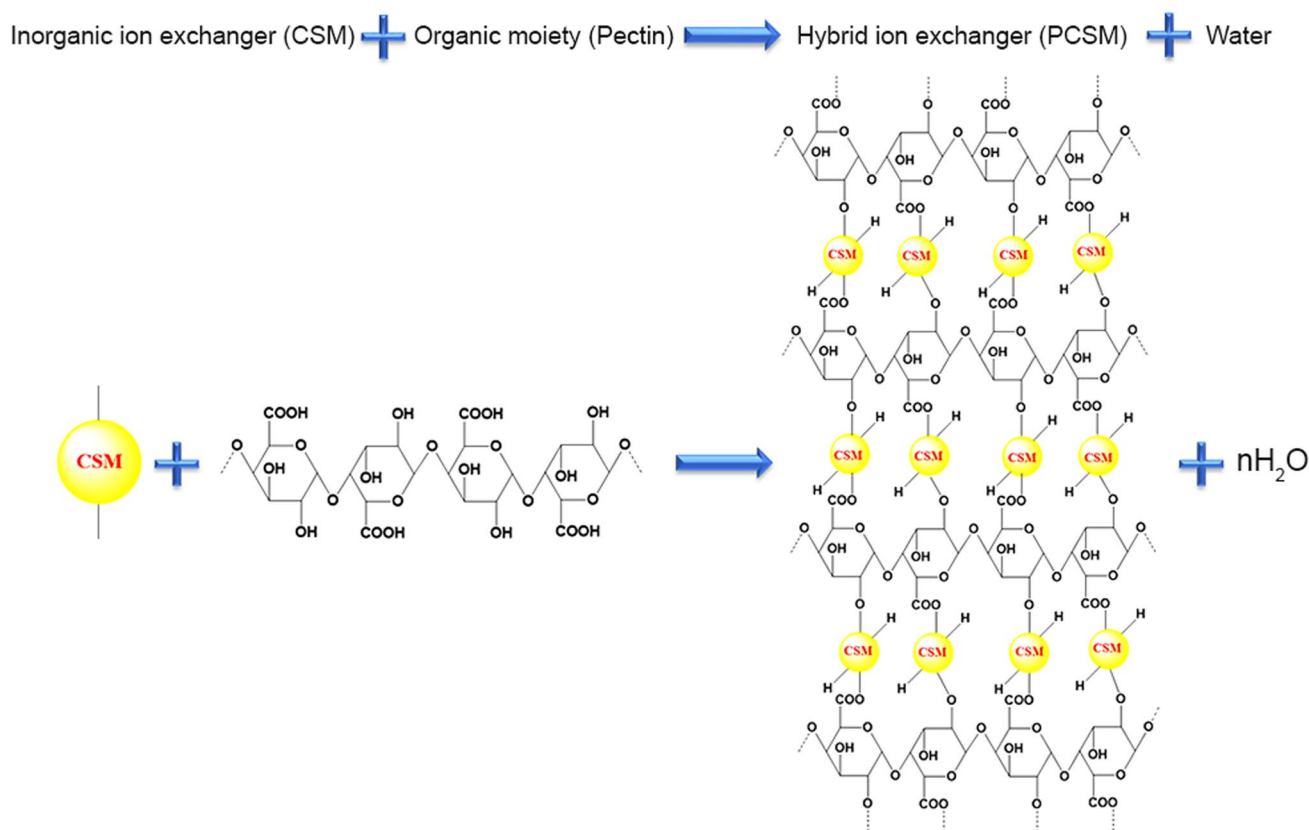


**Fig. 1** Proposed chemical reaction between CSM and pectin for PCSM composite synthesis

function of temperature during a drying process (Table 2). It is observed that as the temperature increases, the IEC decreases due to the organic counterpart's deterioration and the nanocomposite ion exchanger's physical denaturation [24, 34]. By heating up to 600 °C, it is found that the PCSM had average thermal stability as the IEC is now around 24.21% (0.62 meq/g as shown in Table 2) of the initial value (2.56 meq/g given in Table 1).

In the same scenario, eluent concentration-dependent studies were also performed to analyze the suitable concentration of eluent for completely eluting the H<sup>+</sup> ions from the PCSM ion exchanger columns. So, in this experiment, we used various concentrations of NaCl against the m mole of H<sup>+</sup> ions from PCSM. It can be clearly depicted from Fig. 2a that 1 M NaCl is sufficient to completely elute the H<sup>+</sup> ions from the PCSM exchanger column. Furthermore, Fig. 2b shows the maximum volume of NaCl that is required to completely release H<sup>+</sup> ions is 120 mL. This much volume (= 120 mL) of NaCl is indicating the PCSM composite's good performance for complete elution of H<sup>+</sup>

in comparison to many existing pectin-based ion exchangers [26, 31].

It can be clearly observed from Table 3 that the weight of the exchanger is reduced while color may or may not be changed after chemical treatment for 24 h. This table also enlightens that the chemical stability of PCSM is reduced in alkaline solutions as the weight of the exchanger and IEC is reduced. The possible reason behind weaker stability in such strong bases can be the moderated hydrolysis of exchangers at higher pH [24]. Furthermore, the PCSM ion exchanger was found chemically stable in HCl and HNO<sub>3</sub> mineral acids at 0.1, 1.0, and 5.0 M concentrations, and also in CH<sub>3</sub>COOH and CH<sub>3</sub>COCH<sub>3</sub> solvents at 1.0 M concentration.

Now to examine various structural and morphological parameters, we have opted for several characterization techniques. First, various functional groups were detected by observing the FTIR spectra of both CSM and PCSM ion exchangers [42]. Figure 3 shows the FTIR spectra of CSM and PCSM ion exchangers. In the FTIR spectrum of CSM (Fig. 2a), the broadband at 3400.90 cm<sup>-1</sup> with a strong peak

**Table 2** Temperature effects on color and IEC of PCSM ion exchanger

Ion exchanger	Temperature of drying (°C)	Na <sup>+</sup> IEC (meq/g)	Variation in color	% Retention of IEC
Pectin–cerium (IV) silicomolybdate	100	2.05	Faded yellow	80.08
	200	1.97	Blackish gray	76.96
	300	1.68	Dark gray	65.63
	400	1.41	Dark gray	55.08
	500	0.96	Dark brown	37.50
	600	0.62	Dark brown	24.21

Maximum deviation in % retention of IEC at all temperatures is ±2%

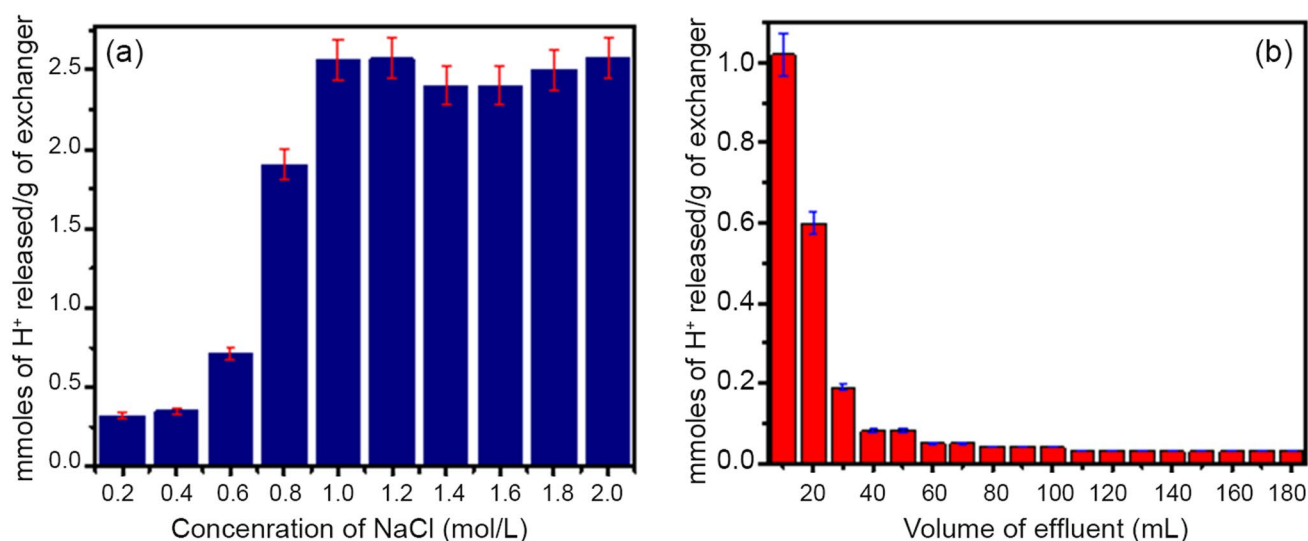


**Fig. 2** a Effect of eluent concentration on PCSM's IEC and b elution behavior of PCSM ion exchanger

**Table 3** Chemical stability of PCSM against different chemicals: effects on PCSM's weight and IEC

Solvents	Wt. before treatment (mg)	Wt. after treatment (mg)	Change in color after treatment	IEC (meq/g)	% Retention of IEC
0.1 M HNO <sub>3</sub>	500	438	No change	2.28	89.06
1.0 M HNO <sub>3</sub>	500	432	No change	2.20	85.94
5.0 M HNO <sub>3</sub>	500	441	No change	2.19	85.55
0.1 M HCl	500	412	No change	2.09	81.64
1.0 M HCl	500	413	No change	2.10	82.03
5.0 M HCl	500	409	No change	2.11	82.42
0.1 M NaOH	500	343	Faded yellow to beige	1.69	66.01
1.0 M NaOH	500	201	Faded yellow to white	1.04	40.62
0.1 M KOH	500	272	Faded yellow to beige	1.38	53.90
1.0 M KOH	500	199	Faded yellow to white	1.03	40.23
1.0 M CH <sub>3</sub> COCH <sub>3</sub>	500	412	No change	2.09	81.64
1.0 MCH <sub>3</sub> COOH	500	436	No change	2.22	86.71

Maximum deviation in % retention of IEC for all solvents is  $\pm 2\%$

at  $1622.64\text{ cm}^{-1}$  is due to the existence of  $-\text{OH}$  bending and stretching modes. Silicate ions are responsible for the peak at  $1084.31\text{ cm}^{-1}$  [43]. A peak at  $961.68\text{ cm}^{-1}$  is clearly indicating the presence of molybdate [17]. The absorption band in the  $567.05\text{ cm}^{-1}$  area may be caused by  $\text{Ce}-\text{O}$  stretching [30]. CSM contains structural hydroxyl protons, as seen by the strong  $1400.45\text{ cm}^{-1}$  band ascribed to the presence of  $\text{Si}-\text{OH}$  [36].

The FTIR spectrum of PCSM shows a peak at  $599.15\text{ cm}^{-1}$  assigned to oxides, and metal hydroxide bands (Fig. 3b) were detected. The  $\text{C}-\text{O}$  stretch of pectin in the PCSM is detected at  $1019.74\text{ cm}^{-1}$  [30] and pectin's  $\text{C}=\text{O}$

double bonds are seen at  $1103.22\text{ cm}^{-1}$  [36]. The band at  $1734.52\text{ cm}^{-1}$  is allocated to the presence of the  $\text{C}=\text{O}$  stretching band of the pectin's ester group [29]. Moreover, the peak at around  $3370.87\text{ cm}^{-1}$  is more or less the same as detected for CSM at  $3400\text{ cm}^{-1}$ . These above results prove the mixing of CSM with pectin without alteration of CSM structure. The presence of pectin peaks and little shift in the peaks of metal oxides and hydroxides in Fig. 3 attest to the formation of PCSM.

The XRD is one of the nondestructive experimental techniques used to characterize the crystalline structure, molecular orientations, grain size, molecular surface, and phase of

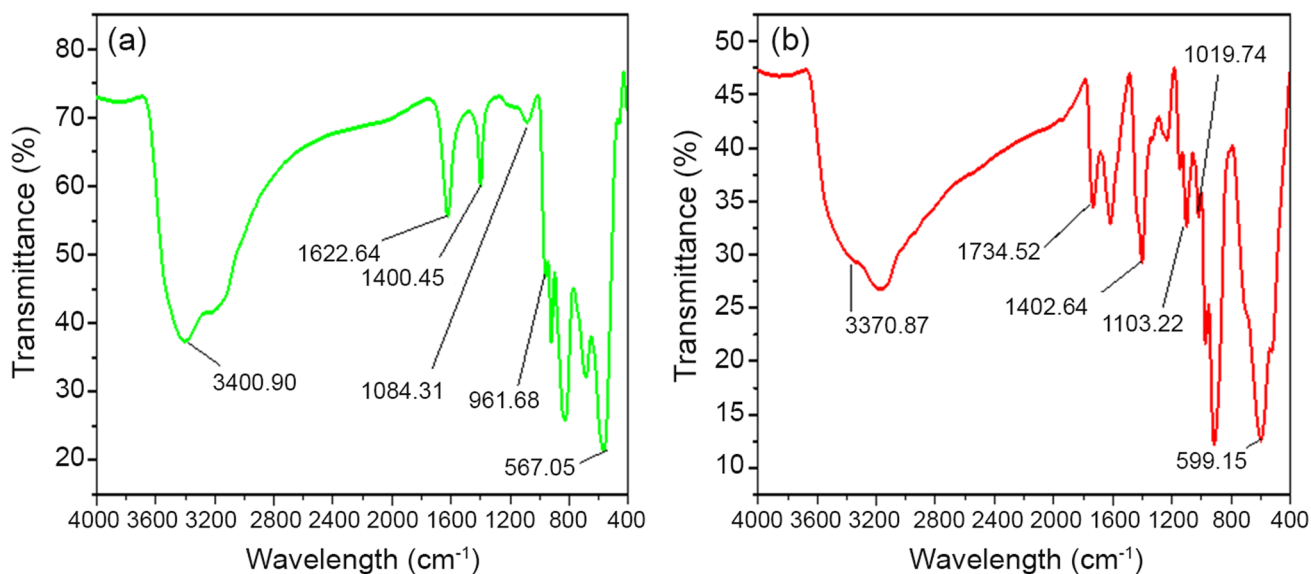


**Fig. 3** FTIR spectra of: **a** CSM, and **b** of PCSM with the designation of various peaks



materials. Henceforth, we have performed powder XRD on PCSM to analyze its crystalline nature. It can be noticed from Fig. 4 that the peaks observed in the PCSM XRD pattern (Fig. 4b) are of low intensities compared to those of the CSM (Fig. 4a). This outcome indicates a decrease in CSM crystallinity when mixed with pectin to form the hybrid PCSM ion exchanger. Indeed, the crystallinity index ( $= \frac{\text{Sum of area under peaks}}{\text{Total area}} \times 100$ ) for CSM was 74.36%, which was then reduced to 56.42% after adding pectin. This result suggests that CSM and PCSM are semi-crystalline materials, with PCSM delineating the lowest crystallinity.

SEM was obtained at different magnifications to observe the morphology of the prepared CSM and PCSM composites (Fig. 5) [44]. It is evident from the SEM images that the PCSM composite has rough morphology with a well-defined flower petal-like structure (Fig. 5c, d). On the other hand, CSM does not have such a structural pattern (Fig. 5a, b). The different surface morphologies between PCSM and CSM hint toward the binding of pectin organic biopolymer with the inorganic ion exchanger material (CSM), and thus confirm the formation of the organic–inorganic PCSM hybrid ion exchanger [17].

The EDX analysis was achieved to examine the elemental compositions of CSM and PCSM composites, and the results are represented in the histogram of Fig. 6 [45]. The EDX analyses were carried out with an SEM and its adjunct EDX analyzer. Ce, Si, Mo, and O components were detected in the EDX spectrum of CSM, indicating that the CSM ion exchanger was synthesized without undesired chemical impurities (Fig. 6a). Peaks corresponding to O and C of the pectin molecular parts were detected in the EDX spectrum of the PCSM coexisting with the peaks of the Ce, Si, Mo,

and O elements confirming the production of the hybrid composite (Fig. 6b).

PCSM particles size was analyzed with the help of TEM images [46]. According to the TEM examination shown in Fig. 7, PCSM composite exhibits particles with an average size in the range 26.2–55.2 nm in at least two dimensions but varying in the third one. On the other hand, the size of particles in the remaining one dimension may vary. Therefore, the PCSM exchanger can also be used as a nano-structured hybrid ion exchanger as two dimensions of the particles are determined to be in the nano-range. This is a very important finding from the industrial application point of view.

Withal the aforesaid characterizations, we have also assessed the selectivity of our composite toward the specific metal ion by analyzing the distribution behavior of the PCSM composite. So, the distribution behavior can be analyzed by observing the ratio of metal ions' amount in the exchanger phase to the amount in the solution phase. One of the prominent methods to calculate this ratio in equilibrium conditions is the measurement of the  $K_d$  value as it gauges the affinity of the cation exchanger toward the counter metal ions. But, the wide variation of  $K_d$  depends not only on the nature of the ion exchanger but also on various other factors such as the type of metal ions, chemical bonds, concentration, pH, and nature of solvents. Therefore, we have performed the distribution studies and measured the  $K_d$  values of 11 metal ions ( $\text{Ba}^{2+}$ ,  $\text{Sr}^{2+}$ ,  $\text{Ca}^{2+}$ ,  $\text{Mg}^{2+}$ ,  $\text{Pb}^{2+}$ ,  $\text{Cd}^{2+}$ ,  $\text{Co}^{2+}$ ,  $\text{Ni}^{2+}$ ,  $\text{Fe}^{3+}$ ,  $\text{Cr}^{3+}$ , and  $\text{Zn}^{2+}$ ) in different solvent systems using the batch method (as shown in Table 4) [47]. Equation (3) may schematically represent the ion exchange reaction process between the PCSM ion exchanger and the metal ions in contact [40].

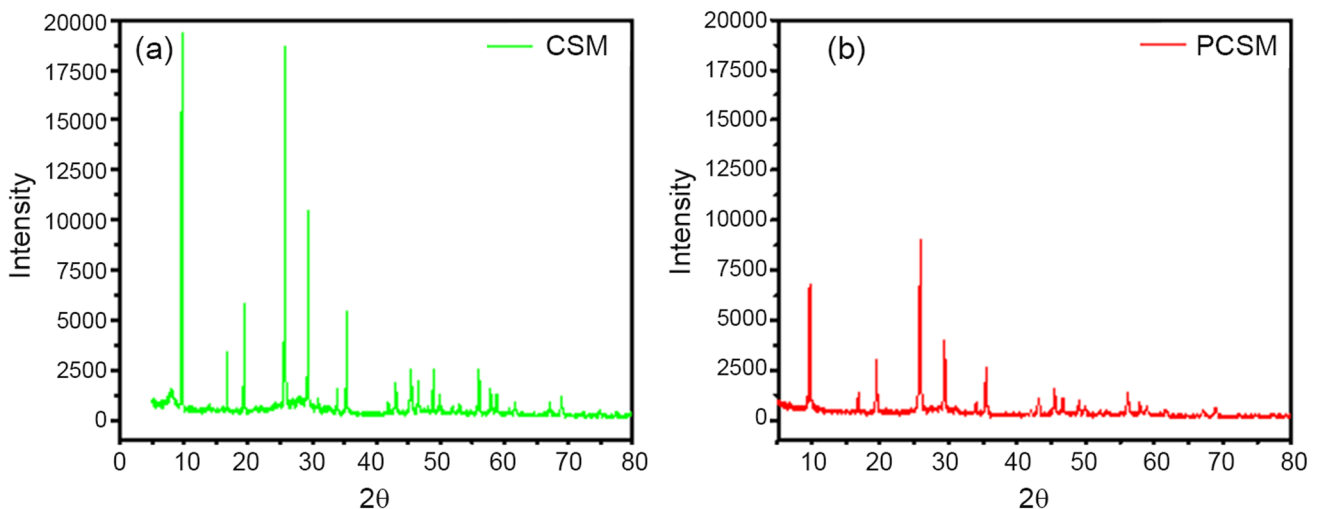


Fig. 4 X-ray diffraction patterns of: **a** CSM and **b** PCSM

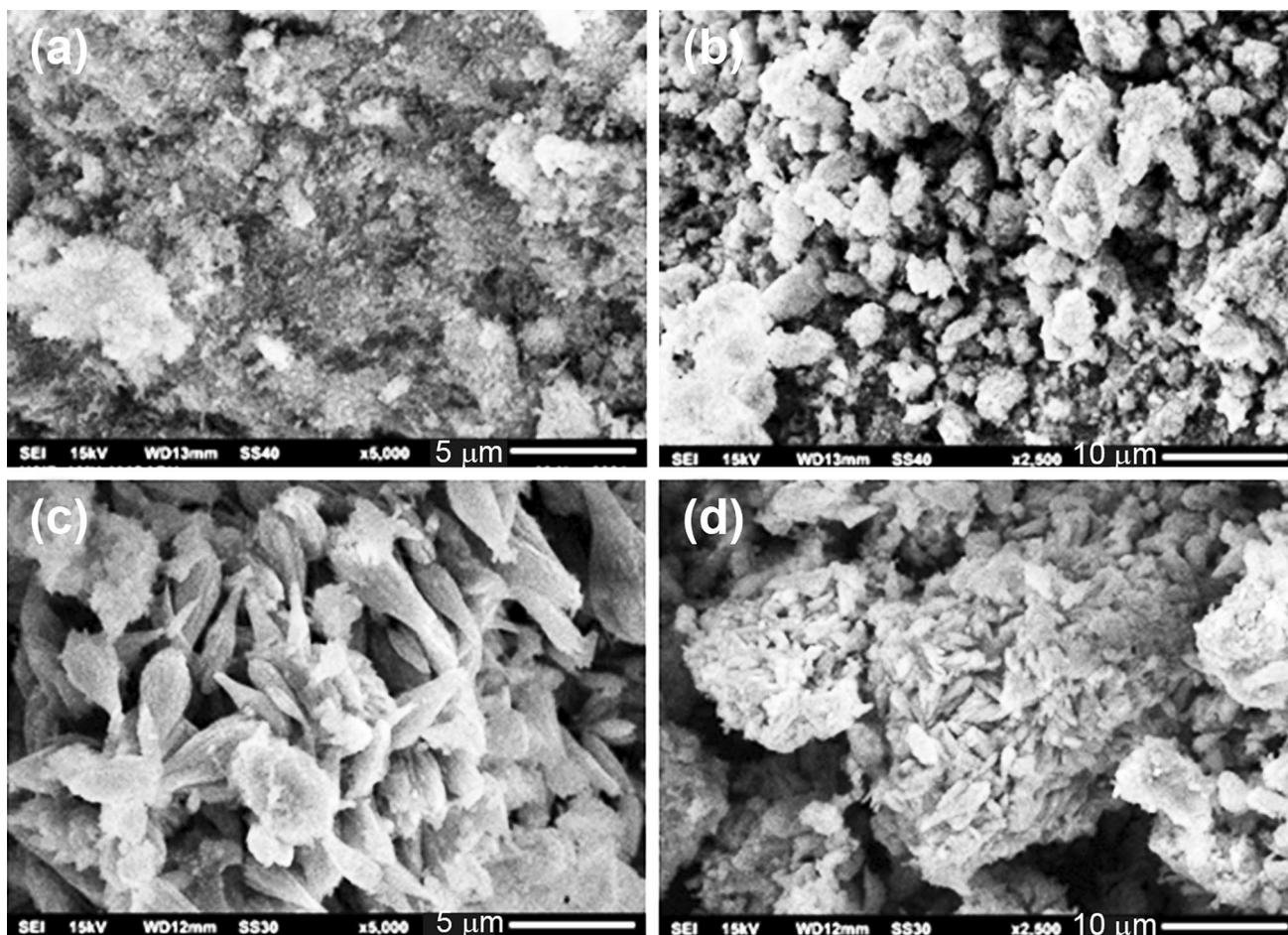


Fig. 5 SEM images of CSM (a, b) and PCSM (c, d) at various magnifications

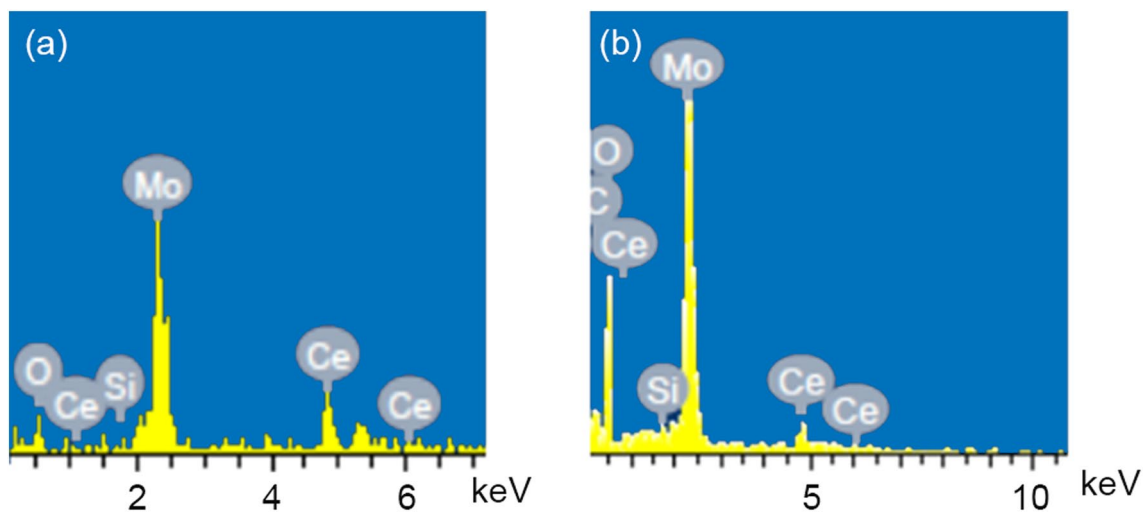
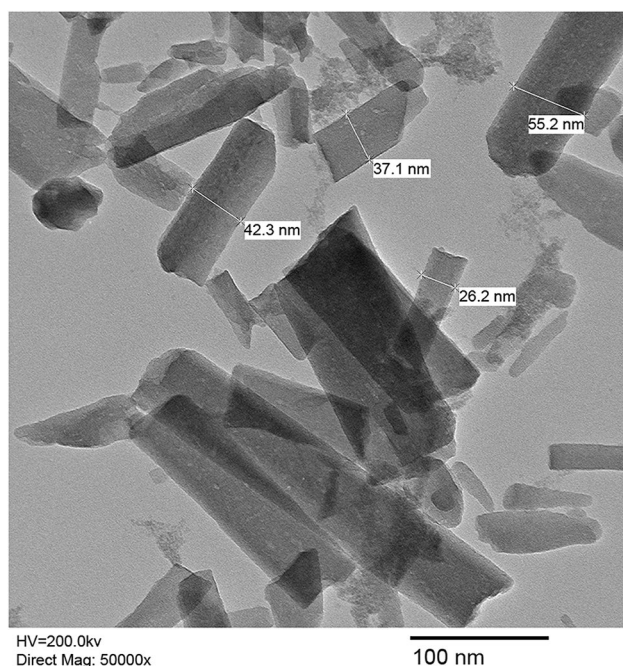


Fig. 6 EDX of: a CSM and b PCSM



**Fig. 7** TEM image of PCSM ion exchanger particles with an average size of the nanoscale range in at least two dimensions



Table 4 shows that some solvents promote the reduction of  $\text{H}^+$  ions from PCSM and show higher sorption of metal ions (i.e., showing high  $K_d$  values), while in some solvents, this process is weak and hence possesses low  $K_d$  values. It can also be observed from Table 4 that mixing two different solvents results in a further decrement of  $K_d$  values in comparison to both solvents individually. This behavior of the

ion exchanger toward the metal ions can be explained on the basis of the higher polarity of mixed solvents in comparison to the individual one. Moreover, this table also revealed that the  $K_d$  values for 0.1 M solvents are lower in comparison to the 0.01 M solvents because of the significant excess of  $\text{H}^+$  ions in 0.1 M solvents which reverted the exchange process, and hence cause the low metal ions pickup [48]. One more promising aspect revealed by this table is the relatively highest  $K_d$  values of PCSM associated with  $\text{Cr}^{3+}$  ions in each of the investigated solvent systems showing, thus, the exchanger's high selectivity for  $\text{Cr}^{3+}$  ions.

By means of different  $K_d$  values of analyzed metal ions, we have also performed the binary separation of metal ions through the batch method. First, to select the suitable pair for binary separation, the separation factor ( $\alpha$ ) was calculated. It is defined as the ratio of  $K_d$  values associated with two different metal ions that are to be separated [49]. So  $\alpha$  can be written as:

$$\alpha = \frac{K_d(\text{A})}{K_d(\text{B})}, \quad (4)$$

where  $K_d(\text{A})$  and  $K_d(\text{B})$  are related to the ionic species A and B that are to be separated sequentially by eluents. For an  $\alpha$  value higher than the unity, the selectivity for ion A is more important than for B. In other words, the higher will be the value of  $\alpha$ , the more effective will be the separation of ion A over B. Based on the value of  $\alpha$  calculated using  $K_d$  of ions in DMW and Eq. (4), we have selected four pairs ( $\text{Cd}^{2+}$ – $\text{Cr}^{3+}$ ,  $\text{Pb}^{2+}$ – $\text{Cr}^{3+}$ ,  $\text{Ni}^{2+}$ – $\text{Cr}^{3+}$ , and  $\text{Co}^{2+}$ – $\text{Cr}^{3+}$ ) of metal ions and associated solutions for binary separations as enlisted in Table 5. Finally, by applying selected eluting agents in succession, metal ions are sequentially eluted through the column to achieve separation. An appropriate

**Table 4**  $K_d$  values of various metal ions present in different solvents on the PCSM column

Metal ions	DMW	0.1 M $\text{HNO}_3$	0.01 M $\text{HNO}_3$	0.1 M $\text{HClO}_4$	0.01 M $\text{HClO}_4$	0.1 M $\text{NaClO}_4$	0.01 M $\text{HClO}_4$ + 0.1 M $\text{NaClO}_4$
$\text{Ba}^{2+}$	93	21	30	55	78	69	65
$\text{Sr}^{2+}$	146	19	42	26	33	63	19
$\text{Ca}^{2+}$	268	28	94	45	68	77	40
$\text{Mg}^{2+}$	316	31	44	43	56	83	33
$\text{Pb}^{2+}$	988	73	261	106	1200	664	511
$\text{Cd}^{2+}$	516	19	87	61	411	218	205
$\text{Co}^{2+}$	455	64	90	12	32	56	10
$\text{Ni}^{2+}$	967	161	168	23	84	140	74
$\text{Fe}^{3+}$	980	68	240	11	536	668	303
$\text{Cr}^{3+}$	1986	189	436	851	2020	619	920
$\text{Zn}^{2+}$	322	14	170	106	336	756	220

All numerical values in this table are the average of three replicate measurements

**Table 5** Separation of binary metal ions systems on PCSM column

Binary mixtures	$\alpha$	Amount loaded (mg)	Amount found (mg)	% Recovery	Eluent used	Eluent volume needed for metal ion elution (mL)
Cd <sup>2+</sup>	3.85	5.62	5.10	90.82	0.1 M HNO <sub>3</sub>	40
Cr <sup>3+</sup>		2.60	2.52	96.99	0.1 M HNO <sub>3</sub>	50
Pb <sup>2+</sup>	2.01	10.35	8.88	85.82	0.1 M HNO <sub>3</sub>	60
Cr <sup>3+</sup>		2.60	2.51	93.05	0.1 M HNO <sub>3</sub>	50
Ni <sup>2+</sup>	2.05	2.93	2.53	86.46	0.1 M HClO <sub>4</sub>	60
Cr <sup>3+</sup>		2.60	2.43	93.46	0.1 M HNO <sub>3</sub>	50
Co <sup>2+</sup>	4.36	2.95	2.75	93.41	0.01 M HClO <sub>4</sub> +0.1 M NaClO <sub>4</sub>	50
Cr <sup>3+</sup>		2.60	2.55	98.23	0.1 M HNO <sub>3</sub>	50

All numerical values in this table are the average of three replicate measurements

eluent is used to elute the weakly held metal ions first, then the stronger ones. Table 4 displays the separation eluents employed and the order of elution. The separations are fairly distinct, and it is observed that recovery is precise and repeatable.

It can also be observed from Table 5 that with increasing the separation factor percentage, recovery of metal ions is also increased and vice versa. As per Table 5, the percentage recovery of Cr<sup>3+</sup> ion ranged from 93.05 to 98.23%. To clearly perceive the behavior of eluting solvent and the amount found after each 10 mL of solvent, we have plotted the volume of 0.01 M EDTA (mL) against the volume of effluent (mL) as shown in Fig. 8. These figures show that the volume of 0.01 M EDTA peaks around 20–30 mL volume of effluent and then gradually decreased.

Apart from the metal ion removal or separation, the synthesized PCSM composite can also be used for antibacterial applications such as the removal of harmful bacteria that normally live in our bodies. One of the common examples of such bacteria is *Escherichia coli* which can be associated with several medical problems like food poisoning, diarrhea, pneumonia, or urinary tract infections. Hence, we have studied the antibacterial properties of PCSM composite against *Escherichia coli* microorganisms using the optical density technique. Figure 9 displays the growth curves of *Escherichia coli* without PCSM (that is designated as negative control) and with various concentrations (50 µg/mL and 100 µg/mL) of PCSM. Herein also, ion exchanger was found to be an effective antibacterial agent

at different concentration levels. The antibacterial property is increased with the increment in the ion exchanger's concentration. It can also be found from Fig. 9 that 100 µg/mL concentration of PCSM decreases the growth rate of bacteria after the incubation of 5 h. One of the possible reasons for the reduction in bacterial growth can be the induction of a relatively prolonged lag phase in the presence of PCSM composite. Hence, PCSM can be effective in the removal of *Escherichia coli* from waterways.

## Conclusion

In this work, a novel nanocomposite ion exchanger was synthesized by precipitation technique using pectin and CSM. The prepared PCSM nanocomposite was characterized and tested for separating heavy metals and eliminating bacterial pollutants from water systems. FTIR results confirmed the association of pectin with CSM and the crystallinity index measurements by XRD characterization revealed the semi-crystalline nature of PCSM. SEM and TEM examinations indicated that PCSM morphology was completely different from that of CSM due to bounding of pectin organic polymer to CSM and its particles were in the nanoscale range at least in two dimensions, respectively. As for metal separation, PCSM exhibited high selectivity toward Cr<sup>3+</sup> ions and also antibacterial activity against Gram-negative bacteria *Escherichia coli*.

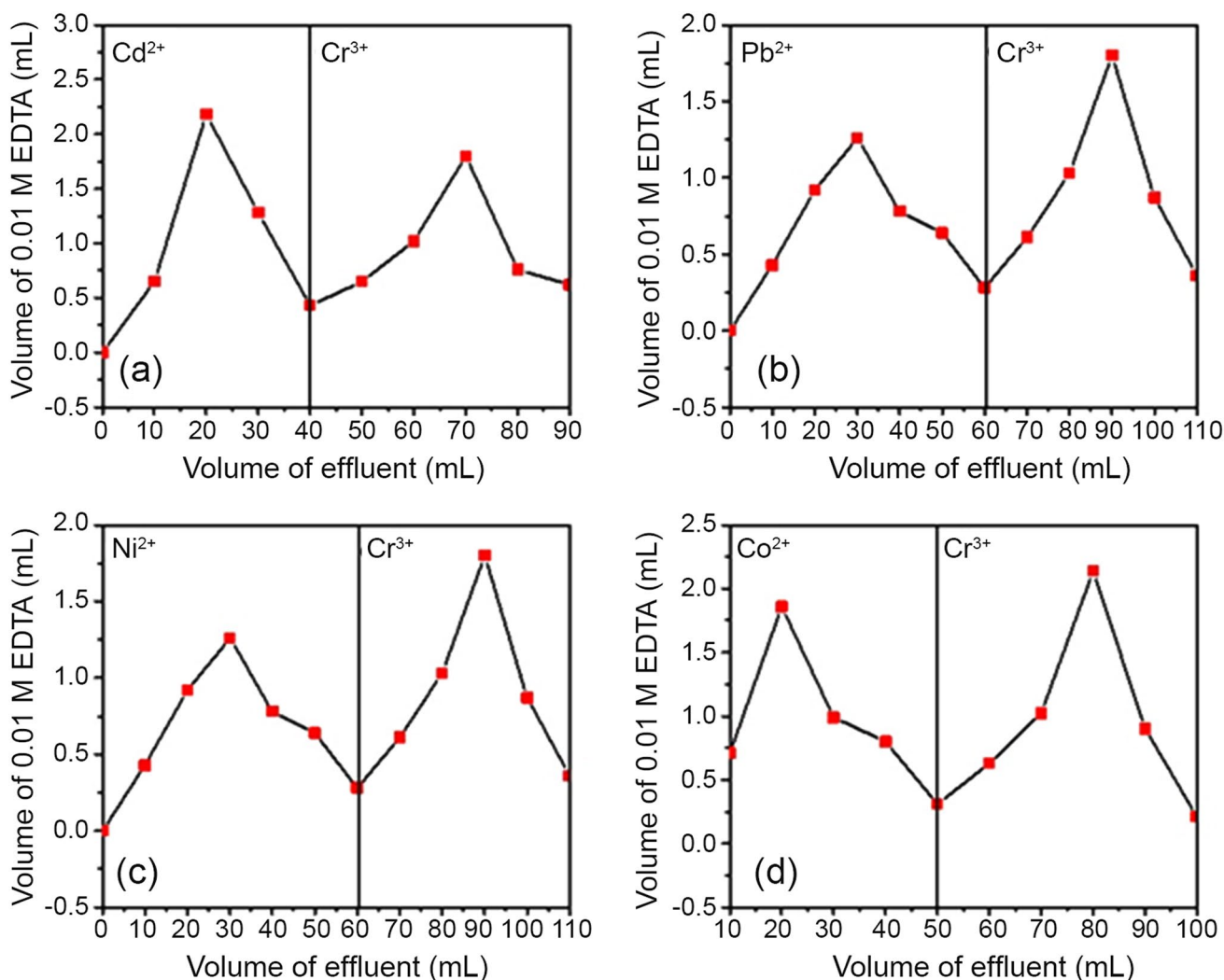


Fig. 8 Chromatograms demonstrating binary separations of metal ions on a PCSM nanocomposite ion exchanger column using different eluents

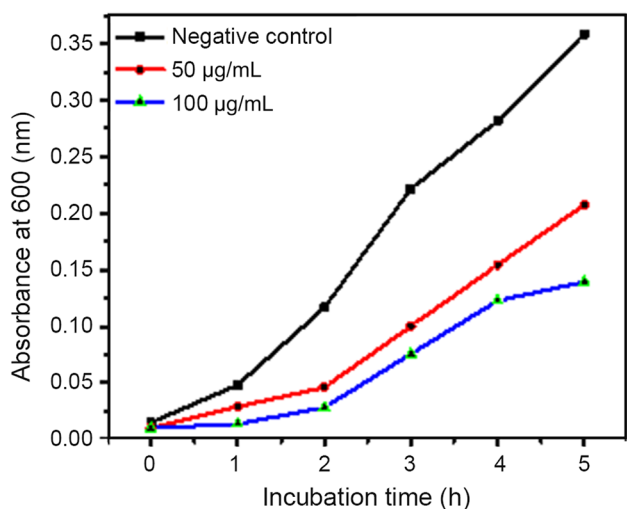


Fig. 9 Growth curve of *Escherichia coli* in the presence of PCSM nanocomposite ion exchanger

**Acknowledgements** The authors are grateful for the research facilities provided by the Chairperson, Department of Chemistry, Aligarh Muslim University Aligarh, India. The writers appreciate the scholarship and contingency funded by University Grants Commission (UGC), New Delhi. One of the authors is grateful for the funds, the UGC start-up grant provided.

**Data availability** The datasets generated during and/or analyzed during the current study are available from the corresponding author upon reasonable request.

**Declarations**

**Conflict of interest** There are no conflicts to declare.

**References**

1. Baban A, Yediler A, Ciliz NK (2010) Integrated water management and CP implementation for wool and textile blend processes.

- Clean: Soil, Air, Water 38:84–90. <https://doi.org/10.1002/clen.200900102>
2. Zaharia C, Suteu D, Muresan A, Muresan R, Popescu A (2009) Textile wastewater treatment by homogeneous oxidation with hydrogen peroxide. *Environ Eng Manag J* 8:1359–1369. <https://doi.org/10.30638/EEMJ.2009.199>
  3. Sekar M, Sakthi V, Rengaraj S (2004) Kinetics and equilibrium adsorption study of lead (II) onto activated carbon prepared from coconut shell. *J Colloid Interface Sci* 279:307–313. <https://doi.org/10.1016/j.jcis.2004.06.042>
  4. Gürkan R, Ulusoy HI, Akçay M (2017) Simultaneous determination of dissolved inorganic chromium species in wastewater/natural waters by surfactant sensitized catalytic kinetic spectrophotometry. *Arab J Chem* 10:S450–S460. <https://doi.org/10.1016/j.arabj.2012.10.005>
  5. Cervantes C, Campos-García J, Devars S, Gutiérrez-Corona F, Loza-Tavera H, Torres-Guzmán JC, Moreno-Sánchez R (2001) Interactions of chromium with microorganisms and plants. *FEMS Microbiol Rev* 25:335–347. [https://doi.org/10.1016/S0168-6445\(01\)00057-2](https://doi.org/10.1016/S0168-6445(01)00057-2)
  6. Shah A, Kluhwar MY, Shah AA (2012) Evaluation of sorption behavior of polymethylene-bis (2-hydroxybenzaldehyde) for Cu(II), Ni(II), Fe(III), Co(II) and Cd(II) ions. *Iran Polym J* 21:325–334. <https://doi.org/10.1007/s13726-012-0033-2>
  7. Akar ST, Akar T, Kaynak Z, Anilan B, Cabuk A, Tabak O, Demir TA, Gedikbey T (2009) Removal of copper (II) ions from synthetic solution and real wastewater by the combined action of dried *Trametes versicolor* cells and montmorillonite. *Hydrometallurgy* 97:98–104. <https://doi.org/10.1016/j.hydromet.2009.01.009>
  8. Amuda OS, Amoo IA (2007) Coagulation/flocculation process and sludge conditioning in beverage industrial wastewater treatment. *J Hazard Mater* 141:778–783. <https://doi.org/10.1016/j.jhazmat.2006.07.044>
  9. Agustina TE, Ang HM, Vareek VK (2005) A review of synergistic effect of photocatalysis and ozonation on wastewater treatment. *J Photochem Photobiol C Photochem Rev* 6:264–273. <https://doi.org/10.1016/j.jphotochemrev.2005.12.003>
  10. Preetha B, Janardan C (2016) Kinetic studies on novel cation exchangers, antimony zirconium phosphate (SbZP) and antimony zirconium triethylammonium phosphate (SbZTP). *Desalination Water Treat* 57:6268–6277. <https://doi.org/10.1080/19443994.2015.1005689>
  11. Varshney KG, Khan MA (2019) Amorphous inorganic ion exchangers. *Inorganic ion exchangers in chemical analysis*. CRC Press, Boca Raton. <https://doi.org/10.1201/9780203750780>
  12. Tiravanti G, Petruzzelli D, Passino R (1997) Pretreatment of tannery waste waters by an ion exchange process for Cr (III) removal and recovery. *Water Sci Technol* 36:197–207. [https://doi.org/10.1016/S0273-1223\(97\)00388-0](https://doi.org/10.1016/S0273-1223(97)00388-0)
  13. Thakur M, Pathania D (2018) Fabrication of gelatin-Zr (IV) phosphate and alginate-Zr (IV) phosphate nanocomposite based ion selective membrane electrode. *Nano Hybrid Compos* 20:108–120. <https://doi.org/10.4028/www.scientific.net/NHC.20.108>
  14. Sharma G, Pathania D, Naushad M (2014) Preparation, characterization and antimicrobial activity of biopolymer based nanocomposite ion exchanger pectin zirconium(IV) selenotungstophosphate: application for removal of toxic metals. *J Ind Eng Chem* 20:4482–4490. <https://doi.org/10.1016/j.jiec.2014.02.020>
  15. Siddiqui WA, Khan SA, Inamuddin (2007) Synthesis, characterization and ion-exchange properties of a new and novel ‘organic-inorganic’ hybrid cation-exchanger: poly(methyl methacrylate) Zr(IV) phosphate. *Colloids Surf A Physicochem Eng Asp* 295:193–199. <https://doi.org/10.1016/j.colsurfa.2006.08.053>
  16. Ahmad N, Kausar A, Muhammad B (2016) Structure and properties of 4-aminobenzoic acid modified polyvinyl chloride and functionalized graphite-based membranes. *Fuller Nanotubes Carbon Nanostructures* 24:75–81. <https://doi.org/10.1080/1536383X.2015.1118620>
  17. Gupta VK, Agarwal S, Pathania D, Kothiyal NC, Sharma G (2013) Use of pectin-thorium (IV) tungstomolybdate nanocomposite for photocatalytic degradation of methylene blue. *Carbohydr Polym* 96:277–283. <https://doi.org/10.1016/j.carbpol.2013.03.073>
  18. Varshney KG, Agrawal A, Mojumdar S (2007) Pyridine based thorium(IV) phosphate hybrid fibrous ion exchanger. *J Therm Anal Calorim* 90:721–724. <https://doi.org/10.1007/s10973-007-8258-6>
  19. Clearfield A (1982) *Inorganic ion exchange materials*. CRC Press, Boca Raton. <https://doi.org/10.1201/9781351073561>
  20. Alam Z, Inamuddin NSA (2010) Synthesis and characterization of a thermally stable strongly acidic Cd(II) ion selective composite cation-exchanger: polyaniline Ce(IV) molybdate. *Desalination* 250:515–522. <https://doi.org/10.1016/j.desal.2008.09.008>
  21. Laiq E, Nabi SA (2021) Preparation, characterization and analytical application of tin (IV) tungstoselenate-1, 10 phenanthroline. *Orient J Chem* 37:997–1001. <https://doi.org/10.13005/oj.370430>
  22. Nataraj SK, Hosamani KM, Aminabhavi TM (2006) Distillery wastewater treatment by the membrane-based nanofiltration and reverse osmosis processes. *Water Res* 40:2349–2356. <https://doi.org/10.1016/j.watres.2006.04.022>
  23. Sirajuddin, Gupta V, Sharma G, Kumar A, Stadler FJ, Inamuddin (2019) Preparation and characterization of gum acacia/Ce(IV) MoPO<sub>4</sub> nanocomposite ion exchanger for photocatalytic degradation of methyl violet dye. *J Inorg Organomet Polym Mater* 29:1171–1183. <https://doi.org/10.1007/s10904-019-01080-9>
  24. Kaur K, Jindal R, Tanwar R (2019) Chitosan-gelatin @ Tin (IV) tungstophosphate nanocomposite ion exchanger: synthesis, characterization and applications in environmental remediation. *J Polym Environ* 27:19–36. <https://doi.org/10.1007/s10924-018-1321-5>
  25. Gupta VK, Agarwal S, Tyagi I, Pathania D, Rathore BS, Sharma G (2015) Synthesis, characterization and analytical application of cellulose acetate-tin (IV) molybdate nanocomposite ion exchanger: binary separation of heavy metal ions and antimicrobial activity. *Ionics* 21:2069–2078. <https://doi.org/10.1007/s11581-015-1368-4>
  26. Gupta VK, Sharma G, Pathania D, Kothiyal NC (2015) Nanocomposite pectin Zr(IV) selenotungstophosphate for adsorptive/photocatalytic remediation of methylene blue and malachite green dyes from aqueous system. *J Ind Eng Chem* 21:957–964. <https://doi.org/10.1016/j.jiec.2014.05.001>
  27. Wang R, Liang R, Dai T, Chen J, Shuai X, Liu C (2019) Pectin-based adsorbents for heavy metal ions: a review. *Trends Food Sci Technol* 91:319–329. <https://doi.org/10.1016/j.tifs.2019.07.033>
  28. Ahmad N, Kausar A, Muhammad B (2016) Perspectives on polyvinyl chloride and carbon nanofiller composite: a review. *Polym Plast Technol Eng* 55:1076–1098. <https://doi.org/10.1080/03602559.2016.1163587>
  29. Gupta VK, Pathania D, Singh P (2014) Pectin-cerium (IV) tungstate nanocomposite and its adsorptive activity for removal of methylene blue dye. *Int J Environ Sci Technol* 11:2015–2024. <https://doi.org/10.1007/s13762-013-0351-8>
  30. Pathania D, Sharma G, Naushad M, Priya V (2016) A biopolymer-based hybrid cation exchanger pectin cerium (IV) iodate: synthesis, characterization, and analytical applications. *Desalination Water Treat* 57:468–475. <https://doi.org/10.1080/19443994.2014.967731>
  31. Pathania D, Sharma G, Thakur R (2015) Pectin @ zirconium (IV) silicophosphate nanocomposite ion exchanger: photocatalysis,

- heavy metal separation and antibacterial activity. *Chem Eng J* 267:235–244. <https://doi.org/10.1016/j.cej.2015.01.004>
32. Laiq E, Shahid N (2021) Antimicrobial activities of Schiff base metal complexes of first transition series. *Biosci Biotechnol Res Asia* 18:575–583. <https://doi.org/10.13005/bbra/2941>
  33. Khan MMA, Rafiuddin I (2014) Synthesis, characterization, thermal behaviour and transport properties of polyvinyl chloride based zirconium phosphate composite membrane. *J Environ Chem Eng* 2:471–476. <https://doi.org/10.1016/j.jece.2014.01.019>
  34. Sharma G, Pathania D, Naushad M, Kothiyal NC (2014) Fabrication, characterization and antimicrobial activity of polyaniline Th(IV) tungstomolybdophosphate nanocomposite material: efficient removal of toxic metal ions from water. *Chem Eng J* 251:413–421. <https://doi.org/10.1016/j.cej.2014.04.074>
  35. Chithra PG, Raveendran R, Beena B (2008) Parachlorophenol anchored tin antimonite: an inorgano-organic ion-exchanger selective towards heavy metals like Bi(III) and Cu(II). *Desalination* 232:20–25. <https://doi.org/10.1016/j.desal.2008.01.006>
  36. Nimisha KV, Mohan A, Janardanann C (2016) Pectin-tin(IV) molybdosilicate: an ecofriendly cationic exchanger and its potential for sorption of heavy metals from aqueous solutions. *Resour Effic Technol* 2:S153–S164. <https://doi.org/10.1016/j.refit.2016.11.016>
  37. Sharma P, Jindal R, Maiti M, Jana AK (2016) Novel organic-inorganic composite material as a cation exchanger from a triterpenoidal system of dammar gum: synthesis, characterization and application. *Iran Polym J* 25:671–685. <https://doi.org/10.1007/s13726-016-0456-2>
  38. Abd El-Latif MM, El-kady MF (2011) Synthesis, characterization and evaluation of nano-zirconium vanadate ion exchanger by using three different techniques. *Mater Res Bull* 46:105–118. <https://doi.org/10.1016/j.materresbull.2010.09.032>
  39. Patel PR, Chudasama UV (2014) Separations of lanthanides and actinides using novel hybrid ion exchange materials, M(IV) phosphonates. *Desalination Water Treat* 52:481–489. <https://doi.org/10.1080/19443994.2013.808796>
  40. Tadesse AM, Ketema TT, Teju E (2020) Cellulose acetate-Sn(IV) molybdophosphate: a biopolymer supported composite exchanger for the removal of selected heavy metal ions. *Bull Chem Soc Ethiop* 34:259–276. <https://doi.org/10.4314/bcse.v34i2.5>
  41. Verma M, Biswal AK, Dhingra S, Gupta A, Saha S (2019) Antibacterial response of polylactide surfaces modified with hydrophilic polymer brushes. *Iran Polym J* 28:493–504. <https://doi.org/10.1007/s13726-019-00717-3>
  42. Ahmad N, Mahmood T (2022) Preparation and properties of 4-aminobenzoic acid-modified polyvinyl chloride/titanium dioxide and PVC/TiO<sub>2</sub> based nanocomposites membranes. *Polym Polym Compos* 30:1–12. <https://doi.org/10.1177/09673911221099301>
  43. Sadeek SA, Ali IM (2016) Polyaniline based cerium phosphosilicate: synthesis, characterization and diffusion mechanism of La (III) in aqueous solutions. *Bull Fac Sci Zagazig Univ* 1:18–35. <https://doi.org/10.21608/bfszu.2016.31063>
  44. Megahed M, Abd El-baky MA, Alsaedy AM, Alshorbagy AE (2021) Synthesis effect of nano-fillers on the damage resistance of GLARE. *Fibers Polym* 22:1366–1377. <https://doi.org/10.1007/s12221-021-0570-4>
  45. Melaihari AA, Attia MA, Abd El-baky MA (2021) Understanding the effect of halloysite nanotubes addition upon the mechanical properties of glass fiber aluminum laminate. *Fibers Polym* 22:1416–1433. <https://doi.org/10.1007/s12221-021-0656-z>
  46. Saber D, Abd El-baky MA, Attia MA (2021) Advanced fiber metal laminates filled with silicon dioxide nanoparticles with enhanced mechanical properties. *Fibers Polym* 22:2447–2463. <https://doi.org/10.1007/s12221-021-0192-x>
  47. Velmurugan G, Ahamed KR, Azarudeen RS (2015) A novel comparative study: synthesis, characterization and thermal degradation kinetics of a terpolymer and its composite for the removal of heavy metals. *Iran Polym J* 24:229–242. <https://doi.org/10.1007/s13726-015-0315-6>
  48. Thakkar R, Chudasama U (2009) Synthesis and characterization of zirconium titanium phosphate and its application in separation of metal ions. *J Hazard Mater* 172:129–137. <https://doi.org/10.1016/j.jhazmat.2009.06.154>
  49. Patel P, Chudasama U (2011) Synthesis and characterization of a novel hybrid cation exchange material and its application in metal ion separations. *Ion Exch Lett* 4:7–15. <https://doi.org/10.3260/iel.2011.06.002>

Springer Nature or its licensor (e.g. a society or other partner) holds exclusive rights to this article under a publishing agreement with the author(s) or other rightsholder(s); author self-archiving of the accepted manuscript version of this article is solely governed by the terms of such publishing agreement and applicable law.